FREFLO: A Macroscopic Simulation Model of Freeway Traffic

Harold J. Payne, ESSCOR, San Diego

Three categories of simulation models for freeway traffic have been developed in the past: microscopic, mesoscopic, and macroscopic. Microscopic models represent individual vehicle movements; mesoscopic models represent platoon movements; and macroscopic models represent traffic flow in terms of aggregate measures such as density, space-mean-speed, and flow rate. This paper discusses a model in the macroscopic category that is particularly useful for evaluating freeway operations. The model is described in mathematical detail for basic flow simulation, ramp metering and diversion, surveillance, and representation of freeway incidents. Computation of performance measures is also detailed. The simulation model, FREFLO, which is based on the model equations presented, is then described and illustrated with a sample run.

A variety of models of traffic flow on highways and freeways has been developed during the past two decades. These models range from analytically tractable car-following models that have limited ability to predict vehicle behavior in real traffic to highly detailed simulation models, of which INTRAS (1) is the most recent and most comprehensive representative. All of these models are at the level of individual vehicle movements and are usually referred to as microscopic.

A second category, macroscopic models, has also been developed (2,3) and is characterized by representations of traffic flow in terms of aggregate measures such as volume (or flow rate), space-mean-speed, and traffic density. This category of model sacrifices a great deal of detail but gains by way of efficiency an ability to deal with problems of much larger scope. There is debate as to whether necessary accuracy is also sacrificed.

There is also a third category of model, mesoscopic. In these, platoons are followed. The SCOT model (4) is the foremost example of this category.

In this paper, we shall discuss a certain subset of the macroscopic model that is, within this category, the most detailed and is capable of representing dynamic behavior well enough to allow study of dynamic traffic operations. We shall, further, describe the related simulation package, FREFLO (5, 6), a successor to the computer simulation package MACK (7).

Figure 1. Aggregate variables.

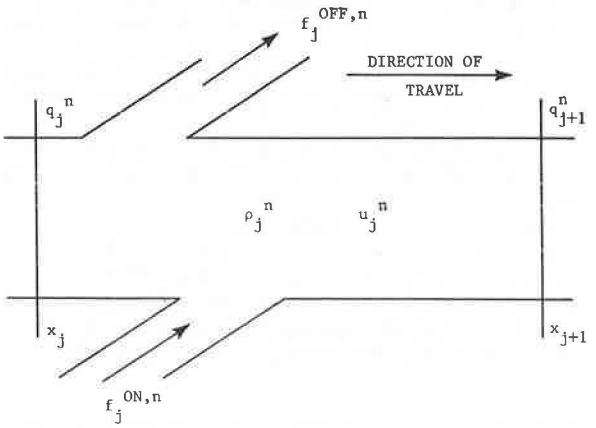

TRAFFIC VARIABLES

The freeway segment is divided into sections, defined by section boundaries at x_j, $j = 1, \ldots, N$. The peak period is divided into uniform time intervals of length Δt. Within the j^{th} section defined by the interval (x_j, x_{j+1}), we shall define the following variables (see Figure 1):

l_j = number of lanes;
Δx_j = section length in kilometers;
ρ_j^n = section density, or number of vehicles in this section at time $t_0 + n\Delta t$ divided by the number of lanes and the section length in vehicles per lane per kilometer; and
u_j^n = section space-mean-speed, or the average of the speeds of the vehicles in section j at time $t_0 + n\Delta t$ in kilometers per hour.

At the section boundary x_j, we define

q_j^n = volume, or the rate at which vehicles pass x_j in the time interval $[t_0 + (n - 1)\Delta t, t_0 + n\Delta t]$ divided by the number of lanes in vehicles per hour per lane,

and, where appropriate,

$f_j^{ON,n}$ = on-ramp volume, or rate at which vehicles enter the on-ramp at x_j in the interval $[t_0 + (n - 1)\Delta t, t_0 + n\Delta t]$ in vehicles per hour, and
$f_j^{OFF,n}$ = off-ramp volume, or rate at which vehicles exit on the off-ramp at x_j in the interval $[t_0 + (n - 1)\Delta t, t_0 + n\Delta t]$ in vehicles per hour.

BASIC MODEL

The first equation expresses the conservation of vehicles:

$$\rho_j^{n+1} = \rho_j^n + (\Delta t / l_j \Delta x_j)(l_{j-1} q_j^{n+1} - l_j q_{j+1}^{n+1} + f_j^{ON,n+1} - f_j^{OFF,n+1}) \quad (1)$$

where $n = 0, 1, 2, \ldots, N$ and $j = 1, \ldots, J$.

Note that we have adopted the convention that a change in the number of lanes is assumed to take place slightly downstream of a section boundary. Consequently, the total freeway volume at x_j is $l_j q_j$. The off-ramp volume is taken to be given by

$$f_j^{OFF,n+1} = \beta_j q_j^{n+1} \quad (2)$$

Under uniform conditions within a section, the volume, density, and speed are related precisely by

$$q_{j+1}^{n+1} = \rho_j^n u_j^n \quad (3)$$

We adopt this as our second equation. The final equation of the model is derived from a continuous-space model by spatial averaging (2).

The dynamic speed-density relationship is

$$u_j^{n+1} = u_j^n - \Delta t \left\{ u_j^n \underbrace{[(u_j^n - u_{j-1}^n)/\Delta x_j]}_{\text{convection}} + 1/T_j \underbrace{[u_j^n - u_e(\rho_j^n)]}_{\substack{\text{relaxation to} \\ \text{equilibrium}}} + (\nu_j/\rho_j^n) \underbrace{[(\rho_{j+1}^n - \rho_j^n)/\Delta x_j]}_{\text{anticipation}} \right\} \quad (4)$$

where j and n proceed as in Equation 1, $T_j = k_T \Delta x_j$, and $\nu_j = k_\nu \Delta x_j$. The parameters k_T and k_ν are termed the relaxation time and anticipation coefficients, respectively. The three groups of terms express three physical processes. The first of these, $[(u_j^n - u_{j-1}^n) \div \Delta x_j]$, is convection, i.e., the fact that vehicles traveling at speed u_{j-1} in the upstream section (section j-1) will tend to continue to travel at that speed as they enter section j. The second, $u_j^n - u_e(\rho_j^n)$, represents the tendency of drivers to adjust their speeds to the equilibrium speed-density relationship. The third, $[(\rho_{j+1}^n - \rho_j^n)/\Delta x_j]$, is a model of anticipation of changing travel conditions ahead; i.e., drivers tend to slow down if the density is seen to be increasing.

In addition, boundary conditions and the initial values of the speeds and densities in each section must be defined. One "dummy" section at each end of the freeway segment is added so that $u_1^n = u_0^n$ and $\rho_1^n = \rho_0^n$.

In the simulations, we have taken

$$u_e(\rho) = \min [88.5 (172 - 3.72\rho + 0.0346\rho^2 - 0.001\,19\rho^3)] \quad (5)$$

where $u_e(\rho)$ is in kilometers per hour. This speed-density relationship is a rescaled version of a least-squares fit to data taken from the Harbor and Hollywood Freeways in Los Angeles (see Figure 2). It is generally necessary to develop a new speed-density relationship for each distinct freeway facility.

Associated with this speed-density relationship, there is a nominal section capacity, defined by

$$c = \max_\rho [\rho u_e(\rho)] \quad (6)$$

This nominal capacity is the largest volume that can be sustained under spatially and temporally uniform conditions. It should be realized, however, that under nonuniform conditions, e.g., in the vicinity of a geometric bottleneck, volumes may exceed nominal capacity.

Note that capacities specific to sections can be obtained by appropriately scaling the speed-density relationship.

Good choices for the parameters k_T and k_ν are 46 s/km (75 s/mile) and 40 km/h (25 mph), respectively (8). The ratio of these parameters to one another is closely related to the phenomenon of slow-down and speed-up cycles in traffic (9). Below the critical speed, u_c, defined by

$$u_c = \sqrt{k_\nu / k_T} \quad (7)$$

traffic, as simulated by the model, exhibits this phenomenon. With the parameters indicated, u_c equals 56 km/h (34.6 mph). Generally, larger values of k_ν and k_T lead to a more sluggish modeled response.

TRAFFIC INCIDENTS

An incident may be reflected in the aggregate variables by (a) a reduction in the number of available lanes, (b) a restriction in the volume flowing past the incident site, and (c) an alteration in parameters such as k_T and k_ν.

The first effect can be represented by placing all vehicles in the affected section in the available lanes. This is manifested as an instantaneous adjustment in density through obvious relationships. The second effect can be represented by noting the expression $q_{j+1}^{n+1} = \rho_j^n u_j^n$ and adjusting the speed u_j^n to limit the flow to the specified volume flowing past the incident site. The third effect has been investigated, but has not proved effective (8).

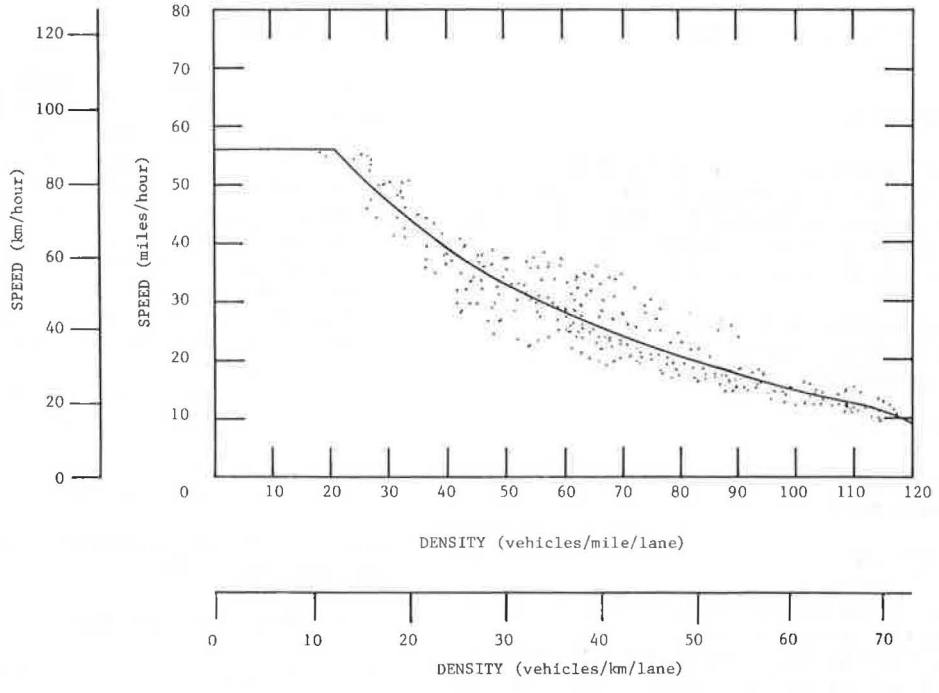

Figure 2. Speed-density relationship.

Figure 3. Modeling of on-ramps.

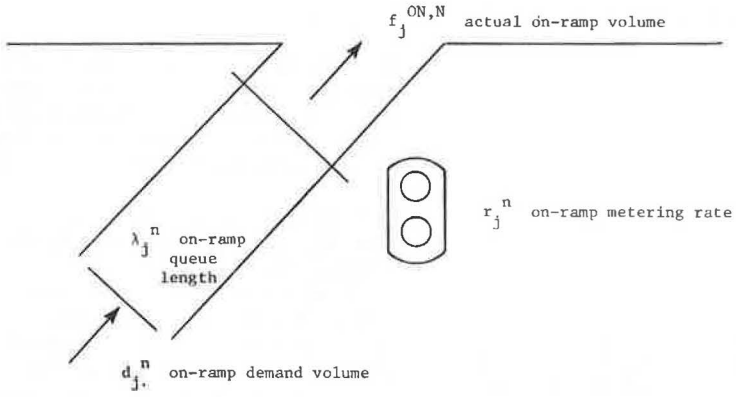

Figure 4. Diversion at on-ramps.

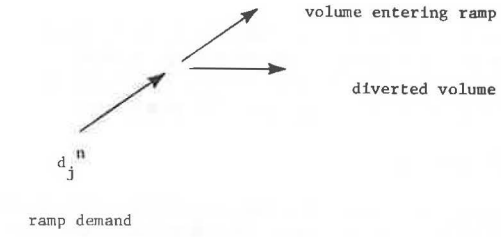

(a) on-ramp variables

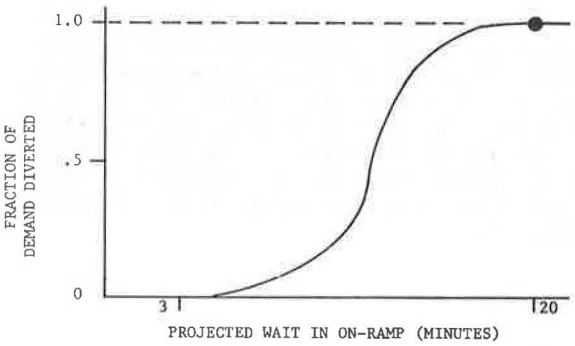

(b) a diversion relationship

ON-RAMP METERING

The variables associated with on-ramp and ramp metering are illustrated in Figure 3. The ramp demand, d_j^n, is metered at the rate r_j^n. When d_j^n exceeds r_j^n, a queue, λ_j^n, is generated. When there is no λ_j^n and d_j^n is less than r_j^n, the actual on-ramp volume, $f_j^{ON,n}$, will equal d_j^n.

In other circumstances, the total demand for the interval Δt can be expressed as $\lambda_j^n/(\Delta t + d_j^n)$; the actual on-ramp rate is then given by

$$f_j^{ON,n} = \min[r_j^n, \lambda_j^n/(\Delta t + d_j^n)] \quad (8)$$

There is now also the need to maintain the queue variable through the expression

$$\lambda_j^{n+1} = \lambda_j^n + (d_j^n - f_j^{ON,n})\Delta t \quad (9)$$

where λ_j^n is the queue length in vehicles on the ramp entering section j at the time $t_0 + n\Delta t$.

As queues build up, there is a tendency for a portion of the drivers arriving at the on-ramp to divert to alternate routes. This effect can be modeled by making this fraction a function of the estimated waiting time, computed as λ_j^n/r_j^n. Figure 4 illustrates the related variables and a candidate diversion relationship. Application of this concept requires that we modify the actual demand on the ramp accordingly.

TRAFFIC CONTROL

Traffic control or ramp metering may be open loop (time of day) or feedback (traffic responsive). In the case of open-loop control, ramp-metering rates are specified for each on-ramp as a function of the time of day. The metering rates function as constraints on the actual on-ramp volume.

With feedback control, the ramp-metering rates depend on traffic conditions as measured by the surveillance system. A local-occupancy feedback mode is illustrated in Figure 5 (10). In this mode, metering rates depend on the occupancy measured at a detector station on a neighboring freeway, usually the station immediately upstream of the ramp. The solid line in Figure 5 applies if the last change in occupancy was positive; the dashed line applies if the last change in occupancy was negative.

We will provide sample outputs involving this ramp-metering scheme in a subsequent section.

SURVEILLANCE

Freeway surveillance is generally accomplished through the use of presence detectors, usually induction loops, placed in each lane of the roadway (8). To simulate occupancy and volume measurements, each measurement is associated with a simulated section. Then the smoothed occupancy is determined from the corresponding section density by a scale factor (here taken as G). The smoothed volume is taken directly from the associated simulated volume.

The smoothing performed in each case is single exponential. The specific formulas are in the form

$$\text{SOCC(time n + 1)} = \text{SOCC(time n)} \times (1 - \alpha) + \alpha \times \text{current density}/G \quad (10)$$

$$\text{SVOL(time n + 1)} = \text{SVOL(time n)} \times (1 - \alpha) + \alpha \times \text{current volume} \quad (11)$$

where α controls the effective time interval over which averaging takes place.

PERFORMANCE MEASURES

Two performance measures generally produced from

Figure 5. Discrete metering rates as a function of percentage occupancy.

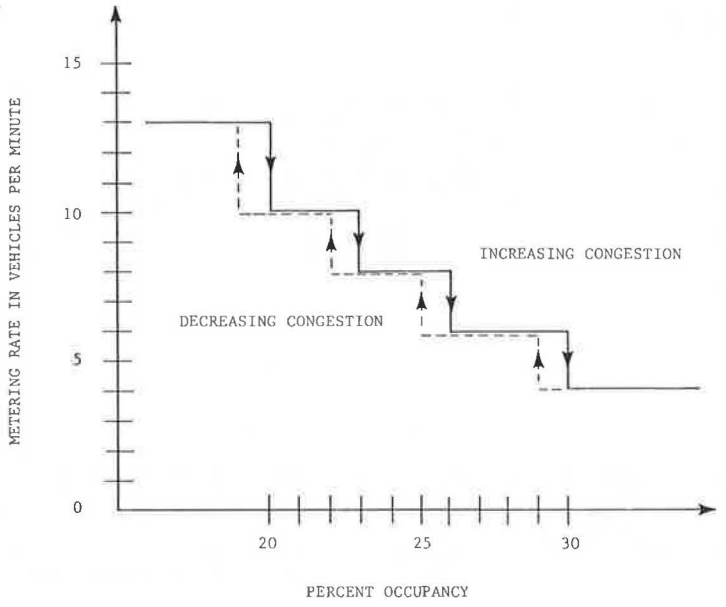

the aggregate variables are service and travel time.

Service

The service rate for the freeway partitioned into sections indexed J = 1, . . . , J is given by

$$\text{total service rate} = \sum_{j=1}^{J} l_j \Delta x_j q_{j+1}^n \tag{12}$$

and has units of vehicle kilometers per hour. The total service performed by the freeway over the time interval $(t_o,\ t_o + N\Delta t)$ is then simply

$$\sum_{n=1}^{N} \sum_{j=1}^{J} l_j \Delta x_j q_{j+1}^n \Delta t \tag{13}$$

and has units of vehicle kilometers.

Travel Time

Total travel time on the freeway is given by the expression

$$\sum_{n=1}^{N} \sum_{j=1}^{J} \ell_j \Delta x_j \rho_j^n \Delta t \tag{14}$$

and has units of vehicle hours. In the presence of ramp queueing, there is a ramp component of total travel time, given by

$$\sum_{n=1}^{N} \sum_{j=1}^{J} \lambda_j^n \Delta t \tag{15}$$

Fuel consumption and pollution emissions are important further measures of performance. Relationships suitable for use with the aggregate variables are not yet firmly established, but some present relationships may be useful and others currently under development certainly will be. Here we shall describe the form the computations take.

Fuel consumption and pollution emissions (HC, CO, NO_x) can be computed for an average automobile from tables (10). Each table provides a rate for a specified speed and acceleration. Thus the total rate for the freeway is in the form

$$\sum_{j=1}^{N} \rho_j^n \ell_j \Delta x_j \times F(u_j^n, a_j^n) \tag{16}$$

where the vehicle acceleration is given by the latter two terms of Equation 3, i.e., the relaxation-to-equilibrium and anticipation terms. Rates for the ramps are also computed from a relationship of the form

$$\sum_{\text{ramps}} \lambda_j^n F(0,0) \tag{17}$$

FREFLO

FREFLO is a FORTRAN program that incorporates all the model features detailed in the following. It is a successor to the program MACK (7). Documentation in the form of a user's guide (5) and program documentation (6) are available.

FREFLO can do the following:

1. Provide a basic model,
2. Perform input data diagnostics,
3. Represent incidents,
4. Model on-ramps,
5. Control time-of-day,
6. Represent surveillance,
7. Represent two traffic-responsive metering modes,
8. Provide standard measures of travel and travel time,
9. Include fuel consumption, and
10. Include pollution emissions.

FREFLO requires such geometric data as number of lanes ℓ_j, j = 1, . . . , d; section lengths Δx_j, j = 1, . . . , d; on-ramp and off-ramp locations; and nominal section capacities. The traffic data it requires are densities $(\rho_1^0, \rho_2^0, \ldots, \rho_N^0)$ and speeds $(u_1^0, u_2^0, \ldots, u_N^0)$ for the initial state, upstream freeway volume $(q_1^n,\ n = 1,2, \ldots, N)$ and on-ramp rates $(f_j^{ON,n},\ n = 1, 2, \ldots, N$ for each section j with an on-ramp) for input volumes and β_j^n n = 1, 2, . . . , N for each section j with an off-ramp for off-ramp fractions.

The simulation parameters of FREFLO are k_ν, an anticipation parameter; k_τ, a relaxation parameter; Δt,

Figure 6. Freeway segment simulated in the example.

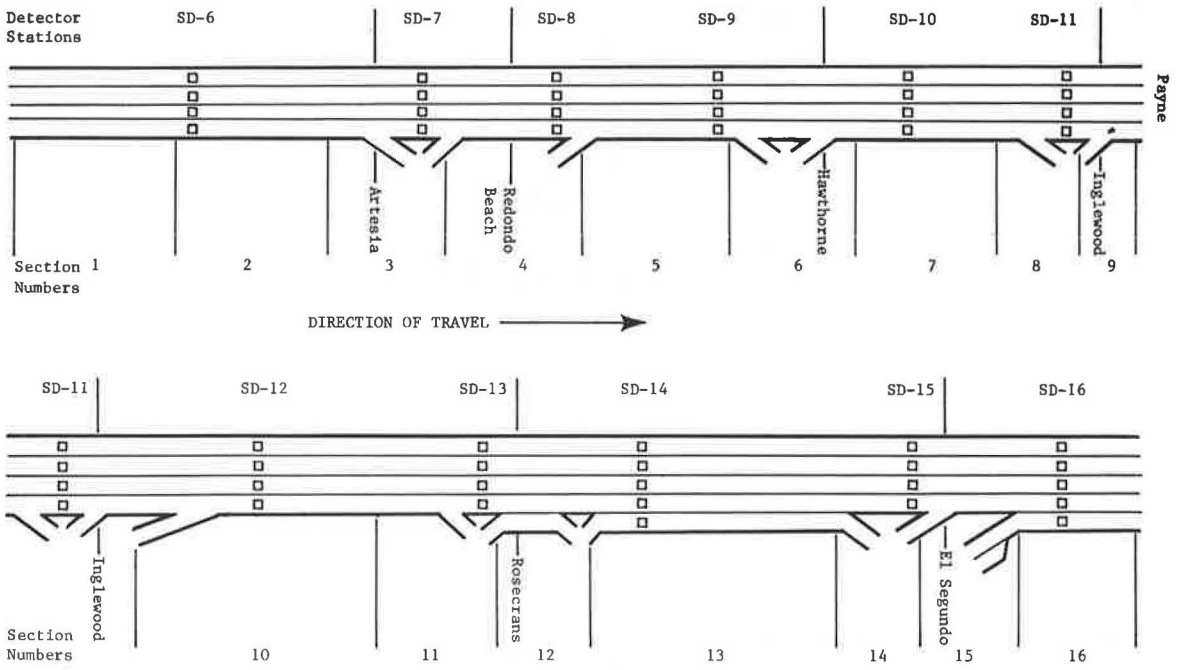

Figure 7. Freeway geometry and link capacities.

FREEWAY GEOMETRY AND LINK CAPACITIES

TOTAL LENGTH	5.40 MI	(8.7 KM)
TOTAL LANE MILES	22.50	(36.2 LANE-KM)
NUMBER OF ON RAMPS	9	
NUMBER OF OFF RAMPS	6	

SECTION NO	LENGTH (MI)	LENGTH (KM)	LANES	SEGMENT CAPACITY (VEH/LN-HR)	ONRAMP CAPACITY (VEH/HR)	OFFRAMP CAPACITY (VEH/HR)
1	0.50	0.80	4	1800.	0.	0.
2	0.40	0.64	4	1800.	0.	0.
3	0.30	0.48	4	1800.	0.	1800.
4	0.30	0.48	4	1800.	1800.	0.
5	0.40	0.64	4	1800.	1800.	0.
6	0.30	0.48	4	1800.	1800.	1800.
7	0.20	0.32	4	1800.	0.	0.
8	0.30	0.48	4	1800.	0.	1800.
9	0.20	0.32	4	1800.	1800.	0.
10	0.40	0.64	4	1800.	1800.	0.
11	0.38	0.61	4	1800.	0.	1800.
12	0.22	0.35	4	1800.	1800.	1800.
13	0.40	0.64	5	1800.	1800.	0.
14	0.38	0.61	4	1800.	0.	1800.
15	0.22	0.35	4	1800.	1800.	0.
16	0.50	0.80	5	1800.	1800.	0.

Figure 8. Initial freeway states.

INITIAL FREEWAY STATES

SECTION NO	INITIAL DENSITY (VEH/LANE-MI)	(VEH/LANE-KM)	INITIAL SPEEDS (MI/HR)	(KM/HR)
1	40.	25.	45.	72.
2	40.	25.	45.	72.
3	40.	25.	45.	72.
4	40.	25.	45.	72.
5	40.	25.	45.	72.
6	40.	25.	45.	72.
7	40.	25.	45.	72.
8	40.	25.	45.	72.
9	40.	25.	45.	72.
10	40.	25.	45.	72.
11	40.	25.	45.	72.
12	40.	25.	45.	72.
13	40.	25.	45.	72.
14	40.	25.	45.	72.
15	40.	25.	45.	72.
16	40.	25.	45.	72.

Figure 9. Simulation parameters and constants and incident scenario.

SIMULATION PARAMETERS AND CONSTANTS

TIMING DATA

INTEGRATION INTERVAL	6.0 SEC
OUTPUT INTERVAL	1.0 MIN
STARTING TIME	730.
ENDING TIME	800.

INTEGRATION CONSTANTS

TEE = 75.0 SEC/MI (46.6 SEC/MI) VEE = 25.0 MI/HR (40.2 KM/HR)

COEFFICIENTS FOR SPEED-DENSITY RELATIONSHIP

0.10700E+03 -0.23100E+01 0.21500E-01 -0.74000E-04

VMAX= 55. MI/HR (88.5 KM/HR)

INCIDENT SCENARIO

INCIDENT SUBINTERVAL	1	2	3
ITH INTERVAL BEGIN TIME	740.	750.	750.
LINK AFFECTED	12	12	0
LANES AVAILABLE	3	4	4
INCIDENT CAPACITY	1600.	1600.	0.

a time step; duration of simulation; and speed-density relationship, $u_e(\rho)$. Its incident scenario parameters include number of lanes available and capacity at incident site. Specifications for its ramp-control parameters depend on choice of mode. Surveillance-data processing parameters are detector-station locations and averaging time. Finally, FREFLO offers the output options of diagnostics only or simulation and a choice of detailed outputs.

SAMPLE SIMULATION

To illustrate the functioning of and outputs provided by FREFLO, we consider an example involving the local occupancy-metering mode with an incident. The freeway segment simulated is illustrated in Figure 6. It is a portion of northbound I-405 in Los Angeles. Figures 7-17, the program printouts, contain the complete input

Figure 10. Output options.

```
OUTPUTS SELECTED INDICATED BY 1

    TIME HISTORY PLOT              0
    TABLES                         1
    SPECIAL DENSITY MAP            1
    SPEED                          1
    DENSITY                        1
    FREEWAY VOLUMES                1
    SERVICE RATES                  0
    ON RAMP DEMANDS                1
    OFF RAMP RATES                 1
    ACTUAL ON RAMP RATES           1
    ONRAMP METERING RATES          1
    ON RAMP QUEUES                 1
    DIVERTED TRAFFIC VOLUMES       1
    ACCELERATIONS                  1
    HC EMISSIONS                   0
    CO EMISSIONS                   0
    NOX EMISSIONS                  0
    FUEL CONSUMPTION               0
    SMOOTHED OCCUPANCY             1
    SMOOTHED VOLUME                1

    SIMULATION TO BE EXECUTED      0

SPATIAL AND TEMPORAL BOUNDS FOR COMPUTATION
OF SUMMARY PERFORMANCE MEASURES
FIRST SECTION       2
LAST SECTION       15
FIRST TIME          0.
LAST TIME        9999.
```

Figure 11. Surveillance and diversion parameters.

```
SURVEILLANCE DATA PARAMETERS

AVERAGING TIME              60. SEC
SMOOTHING CONSTANT          .1000
G-FACTOR                   2.5000
DETECTOR STATIONS/SECTION CORRESPONDENCE

DETECTOR          SECTION FOR
STATION           OCC   VOL
   1                1     1
   2                1     1
   3                1     1
   4                1     1
   5                1     1
   6                2     3
   7                3     4
   8                4     5
   9                5     6
  10                7     8
  11                8     9
  12               10    11
  13               11    12
  14               13    14
  15               14    15
  16               16    17
DIVERSION PARAMETERS
DIVP1 =    3.00
DIVP2 =   20.00
DIVP3 =    0.00
```

Figure 12. Ramp-metering plan parameters.

```
RAMP METERING PLAN PARAMETERS

METERING MODE  2 SELECTED
PARAMETERS FOR LOCAL OCCUPANCY PLAN

NUMBER OF METERING LEVELS      6
UPDATE INTERVAL                1.00 MIN

ON RAMP   CONTROLLING
        DETECTOR STATION

    4          7
    5          8
    6          9
    9         11
   10         11
   12         13
   13         14
   15         15
   16         15

OCCUPANCY THRESHOLDS      METERING RATE IF
     (PER CENT)           GREATER THAN THRESHOLD
INCREASING DECREASING          (VEH/HR)

                               1800.
    15.        15.             780.
    20.        20.             600.
    23.        23.             480.
    26.        26.             360.
    30.        30.             240.
```

Figure 13. Traffic demand data.

```
TRAFFIC DEMANDS BEGINNING AT    730.

UPSTREAM FREEWAY VOLUME    7116.  VEH/HR
 SECTION NO  ONRAMP   OFFRAMP
             VOLUME   FRACTION
            (VEH/HR)

      1         0.      0.000
      2         0.      0.000
      3         0.      0.046
      4       288.      0.000
      5       372.      0.000
      6       624.      0.034
      7         0.      0.000
      8         0.      0.102
      9       420.      0.000
     10       168.      0.000
     11         0.      0.019
     12       636.      0.093
     13       960.      0.000
     14         0.      0.110
     15       180.      0.000
     16       732.      0.000
```

Figure 14. Summary simulation results.

```
SIMULATION RESULTS

TOTAL TRAVEL TIME                  0.5104E+03 VEHICLE-HOURS
TOTAL FREEWAY TRAVEL TIME          0.4804E+03 VEHICLE-HOURS
TOTAL RAMP QUEUE WAITING TIME      0.2998E+02 VEHICLE-HOURS
TOTAL SERVICE                      0.1508E+05 VEHICLE-MILES
                                  (0.9370E+04 VEHICLE-KMS)
TOTAL DIVERTED VOLUME              0.4264E+03 VEHICLES


                                     TOTAL      FREEWAY      RAMPS
HC EMISSIONS (GMS X 100)         0.2957E+03 0.2751E+03 0.2057E+02
CO EMISSIONS (GMS X 100)         0.3623E+04 0.3216E+04 0.4071E+03
NOX EMISSIONS (GMS X 100)        0.7549E+03 0.7265E+03 0.2838E+02
FUEL CONSUMPTION (GALS)          0.1162E+04 0.1104E+04 0.5780E+02
                 (LITERS)        0.4398E+04 0.4179E+04 0.2188E+03
```

Figure 15. Detailed simulation results on speed.

SPEED(MI/HR)*

	SECTION INDEX →															
TIME	1	2	3	4	5	6	7	8	9	10	11	12	13	14	15	16
730.	45.	45.	45.	45.	45.	45.	45.	45.	45.	45.	45.	45.	45.	45.	45.	45.
731.	44.	45.	45.	43.	43.	43.	44.	44.	44.	44.	45.	46.	45.	43.	44.	45.
732.	45.	45.	45.	43.	41.	41.	43.	44.	44.	44.	45.	46.	46.	44.	44.	46.
733.	45.	45.	44.	43.	40.	40.	41.	43.	43.	44.	45.	47.	46.	45.	45.	47.
734.	45.	45.	44.	42.	40.	39.	40.	42.	42.	43.	45.	47.	47.	45.	46.	47.
735.	45.	45.	44.	42.	39.	38.	39.	41.	42.	43.	45.	47.	47.	46.	47.	48.
736.	45.	45.	44.	42.	39.	37.	39.	40.	41.	42.	44.	47.	47.	46.	47.	49.
737.	45.	45.	44.	41.	38.	37.	38.	39.	40.	41.	44.	47.	47.	47.	48.	49.
738.	45.	45.	44.	41.	38.	36.	37.	39.	39.	41.	44.	46.	47.	47.	48.	50.
739.	45.	45.	44.	41.	37.	36.	37.	38.	39.	40.	43.	46.	47.	47.	48.	50.
740.	45.	45.	44.	41.	37.	35.	36.	37.	38.	40.	43.	46.	47.	47.	49.	50.
741.	45.	45.	43.	40.	36.	35.	36.	37.	38.	38.	27.	19.	37.	45.	50.	51.
742.	45.	45.	43.	40.	36.	34.	35.	36.	36.	33.	19.	16.	37.	47.	52.	53.
743.	45.	45.	43.	40.	36.	34.	35.	35.	34.	27.	15.	14.	37.	47.	52.	53.
744.	44.	45.	43.	40.	35.	33.	34.	34.	31.	23.	13.	13.	36.	47.	52.	53.
745.	44.	45.	43.	39.	35.	33.	33.	32.	28.	19.	12.	13.	36.	47.	52.	53.
746.	44.	45.	43.	39.	34.	32.	32.	29.	24.	17.	11.	12.	36.	47.	52.	53.
747.	44.	44.	42.	39.	34.	31.	30.	26.	21.	15.	10.	12.	36.	47.	52.	53.
748.	44.	44.	42.	38.	33.	30.	28.	23.	19.	13.	10.	13.	36.	47.	52.	53.
749.	44.	44.	42.	38.	32.	28.	26.	21.	17.	12.	9.	13.	36.	47.	52.	53.
750.	44.	44.	42.	37.	31.	27.	24.	18.	15.	10.	9.	13.	36.	47.	52.	53.
751.	44.	44.	41.	36.	30.	25.	22.	16.	13.	10.	19.	28.	40.	49.	54.	54.
752.	44.	44.	41.	35.	28.	23.	20.	14.	12.	14.	23.	30.	38.	45.	51.	53.
753.	44.	43.	40.	34.	26.	20.	18.	13.	13.	18.	25.	32.	38.	43.	48.	51.
754.	44.	43.	39.	32.	24.	19.	17.	14.	15.	20.	26.	32.	38.	42.	47.	50.
755.	43.	43.	38.	30.	22.	18.	17.	16.	18.	21.	28.	33.	38.	42.	46.	49.
756.	43.	42.	36.	28.	20.	18.	18.	17.	19.	23.	28.	34.	38.	42.	45.	49.
757.	43.	41.	35.	26.	20.	18.	19.	19.	20.	23.	29.	35.	39.	42.	45.	48.
758.	42.	40.	33.	25.	20.	19.	20.	20.	21.	24.	30.	36.	39.	42.	45.	48.
759.	42.	39.	32.	24.	20.	19.	20.	21.	22.	25.	31.	37.	40.	42.	45.	48.
800.	41.	38.	31.	24.	20.	20.	21.	21.	23.	26.	32.	37.	40.	43.	45.	48.

Figure 16. Detailed simulation results on on-ramp metering rates.

ON RAMP METERING RATES(VEH/HR)

SECTION INDEX →

TIME	1	2	3	4	5	6	7	8	9	10	11	12	13	14	15	16
730.	1800.	1800.	1800.	1800.	1800.	1800.	1800.	1800.	1800.	1800.	1800.	1800.	1800.	1800.	1800.	1800.
731.	0.	0.	0.	780.	780.	780.	0.	0.	780.	780.	0.	780.	780.	0.	780.	780.
732.	0.	0.	0.	780.	780.	780.	0.	0.	780.	780.	0.	780.	780.	0.	780.	780.
733.	0.	0.	0.	780.	780.	780.	0.	0.	780.	780.	0.	780.	780.	0.	780.	1800.
734.	0.	0.	0.	780.	780.	780.	0.	0.	780.	780.	0.	780.	780.	0.	780.	1800.
735.	0.	0.	0.	780.	780.	780.	0.	0.	780.	780.	0.	780.	780.	0.	780.	1800.
736.	0.	0.	0.	780.	780.	780.	0.	0.	780.	780.	0.	780.	780.	0.	780.	1800.
737.	0.	0.	0.	780.	780.	780.	0.	0.	780.	780.	0.	780.	780.	0.	780.	1800.
738.	0.	0.	0.	780.	780.	780.	0.	0.	780.	780.	0.	780.	780.	0.	780.	1800.
739.	0.	0.	0.	780.	780.	780.	0.	0.	780.	600.	0.	780.	780.	0.	1800.	1800.
740.	0.	0.	0.	780.	780.	780.	0.	0.	780.	600.	0.	780.	780.	0.	1800.	1800.
741.	0.	0.	0.	780.	780.	780.	0.	0.	780.	600.	0.	780.	780.	0.	1800.	1800.
742.	0.	0.	0.	780.	780.	780.	0.	0.	600.	600.	0.	780.	780.	0.	1800.	1800.
743.	0.	0.	0.	780.	780.	780.	0.	0.	600.	600.	0.	780.	600.	0.	1800.	1800.
744.	0.	0.	0.	780.	780.	780.	0.	0.	600.	600.	0.	600.	360.	0.	1800.	1800.
745.	0.	0.	0.	780.	780.	780.	0.	0.	600.	600.	0.	480.	240.	0.	1800.	1800.
746.	0.	0.	0.	780.	780.	780.	0.	0.	600.	600.	0.	360.	240.	0.	1800.	1800.
747.	0.	0.	0.	780.	780.	780.	0.	0.	600.	600.	0.	240.	240.	0.	1800.	1800.
748.	0.	0.	0.	780.	780.	780.	0.	0.	600.	480.	0.	240.	240.	0.	1800.	1800.
749.	0.	0.	0.	780.	780.	780.	0.	0.	600.	480.	0.	240.	240.	0.	1800.	1800.
750.	0.	0.	0.	780.	780.	780.	0.	0.	600.	360.	0.	240.	240.	0.	1800.	1800.
751.	0.	0.	0.	780.	780.	780.	0.	0.	600.	360.	0.	240.	240.	0.	1800.	1800.
752.	0.	0.	0.	780.	780.	780.	0.	0.	480.	360.	0.	240.	240.	0.	1800.	1800.
753.	0.	0.	0.	780.	780.	780.	0.	0.	480.	240.	0.	240.	240.	0.	1800.	1800.
754.	0.	0.	0.	780.	780.	780.	0.	0.	480.	240.	0.	240.	240.	0.	1800.	1800.
755.	0.	0.	0.	780.	780.	780.	0.	0.	360.	240.	0.	240.	240.	0.	780.	1800.
756.	0.	0.	0.	780.	780.	780.	0.	0.	360.	240.	0.	240.	240.	0.	780.	1800.
757.	0.	0.	0.	780.	780.	780.	0.	0.	240.	240.	0.	240.	360.	0.	780.	1800.
758.	0.	0.	0.	780.	780.	780.	0.	0.	240.	240.	0.	240.	360.	0.	780.	1800.
759.	0.	0.	0.	780.	780.	780.	0.	0.	240.	240.	0.	240.	360.	0.	780.	1800.
800.	0.	0.	0.	780.	780.	780.	0.	0.	240.	240.	0.	240.	480.	0.	780.	1800.

Figure 17. Detailed simulation results on CO emissions.

CO EMISSIONS(GM X 100/HR)

SECTION INDEX →

TIME	1	2	3	4	5	6	7	8	9	10	11	12	13	14	15	16
730.	0.	0.	0.	0.	0.	0.	0.	0.	0.	0.	0.	0.	0.	0.	0.	0.
731.	451.	359.	261.	303.	420.	356.	189.	253.	224.	387.	342.	270.	516.	353.	228.	606.
732.	452.	362.	259.	304.	426.	363.	197.	257.	224.	385.	340.	267.	537.	348.	227.	600.
733.	451.	361.	259.	306.	431.	369.	201.	263.	226.	387.	338.	268.	560.	343.	226.	596.
734.	451.	361.	260.	308.	438.	370.	206.	269.	229.	389.	338.	266.	583.	340.	223.	591.
735.	451.	361.	259.	307.	441.	376.	210.	272.	228.	395.	340.	266.	608.	336.	220.	589.
736.	450.	361.	260.	309.	443.	381.	213.	278.	230.	398.	343.	266.	630.	333.	218.	584.
737.	450.	361.	260.	309.	448.	384.	217.	282.	233.	402.	344.	267.	653.	329.	218.	584.
738.	450.	362.	261.	311.	453.	389.	221.	286.	234.	408.	346.	268.	678.	329.	216.	583.
739.	450.	357.	262.	310.	457.	393.	223.	290.	235.	411.	350.	267.	703.	328.	217.	577.
740.	450.	358.	261.	311.	458.	397.	226.	295.	238.	416.	354.	268.	724.	328.	216.	582.
741.	450.	358.	261.	313.	462.	400.	229.	299.	240.	420.	425.	412.	651.	258.	184.	556.
742.	451.	358.	262.	314.	466.	404.	232.	302.	243.	452.	607.	520.	783.	236.	165.	498.
743.	451.	359.	263.	316.	470.	407.	235.	309.	250.	517.	775.	600.	802.	228.	160.	473.
744.	451.	359.	264.	315.	474.	412.	239.	319.	264.	612.	924.	676.	830.	220.	155.	458.
745.	452.	360.	265.	317.	478.	416.	245.	335.	286.	725.	1046.	574.	826.	214.	151.	447.
746.	452.	360.	265.	318.	482.	422.	252.	360.	318.	846.	1140.	620.	838.	212.	150.	441.
747.	452.	361.	266.	318.	488.	429.	263.	395.	357.	962.	1221.	669.	847.	211.	149.	438.
748.	450.	362.	267.	320.	495.	441.	278.	440.	402.	1070.	1294.	718.	853.	211.	149.	438.
749.	451.	360.	267.	323.	505.	456.	299.	498.	450.	1182.	1364.	750.	857.	211.	149.	437.
750.	451.	361.	269.	326.	518.	477.	324.	563.	502.	1322.	1421.	908.	866.	211.	149.	438.
751.	452.	362.	269.	329.	539.	510.	355.	638.	568.	1421.	982.	642.	902.	287.	187.	473.
752.	453.	363.	270.	335.	564.	546.	396.	726.	628.	1274.	739.	640.	933.	322.	202.	531.
753.	454.	363.	274.	344.	602.	596.	440.	794.	621.	1038.	675.	640.	934.	336.	208.	546.
754.	455.	365.	277.	356.	648.	648.	472.	795.	558.	907.	628.	647.	933.	348.	213.	556.
755.	453.	368.	282.	372.	705.	689.	480.	738.	509.	834.	595.	651.	928.	350.	217.	566.
756.	455.	370.	289.	394.	760.	705.	465.	681.	480.	785.	569.	654.	922.	351.	218.	569.
757.	458.	373.	300.	421.	791.	708.	449.	635.	469.	745.	548.	655.	965.	352.	219.	570.
758.	458.	377.	312.	446.	815.	696.	436.	604.	472.	711.	526.	654.	989.	351.	220.	575.
759.	462.	382.	324.	462.	826.	686.	423.	575.	477.	686.	508.	652.	1006.	347.	219.	577.
800.	465.	388.	336.	478.	831.	677.	411.	550.	484.	659.	493.	652.	1046.	347.	219.	577.

and selected outputs. Full examples of the runs, which were carried out in miles originally, are available in the user's guide (5).

From Figure 7 it can be seen that the simulated segment consists of 16 sections that range in length from 0.3 to 0.8 km (0.2 to 0.5 miles), and have four or five lanes each. Nominal section capacities are taken to be 1800 vehicles/lane-h.

From Figure 9 it can be seen that the simulation covers the half-hour interval between 7:30 and 8:00 and involves an incident. This incident occurs in section 12, lasts from 7:40 to 7:50, reduces the number of available lanes to three (from four), and reduces the nominal capacity to 1600 vehicles/lane-h.

Figure 10 details the relationship between detector stations and sections, also illustrated in Figure 6. Figure 12 provides details of the ramp-metering plan. The plan selected was the local occupancy plan, as illustrated in Figure 5.

Traffic demand data are provided in Figure 13. The indicated off-ramp fractions are to be associated with the parameters β_i defined earlier.

Summary simulation results are provided in Figure 14. The remaining Figures 15-17 provide three of the available detailed outputs. Each of the detailed outputs is in the form of an array of values specific to a time instant and section. In the figures, values are provided at 1-min intervals. The effects of the incident are clearly in these detailed outputs as reduced speeds (Figure 15), reduced metering rates (Figure 16), and

increased CO emissions (Figure 17).

CONCLUSION

The macroscopic simulation model as represented by FREFLO has undergone only limited calibration and validation but has shown considerable promise (8). Present research is involved in further validation efforts and will be the subject of a future paper.

Applications of the model described here have been made in several studies of the development and evaluation of ramp-metering strategies (12, 13). FREFLO is currently being used in two national studies. The first of these is a Federal Highway Administration study on control strategies in response to freeway incidents; the second is a study concerned with analytic and field evaluations of ramp-metering strategies.

REFERENCES

1. D. A. Wicks and E. B. Lieberman; KLD Associates. Development and Testing of INTRAS, a Microscopic Freeway Simulation Model: Volume 1—Program Design, Parameter Calibration and Freeway Dynamics Component Development. Federal Highway Administration, Rept. FHWA-RD-76-76, May 1977.
2. H. J. Payne. Models of Freeway Traffic and Control. Simulation Council Proc., Mathematics of Public Systems, Vol. 1, No. 1, 1971, pp. 51-61.
3. M. P. Orthlieb, S. Roedder, and A. May. Freeway Operations Study: Phase III—Progress Toward a Freeway Corridor Model. Institute of Transportation and Traffic Engineering, Univ. of California, Berkeley, Rept. 73-4, Sept. 1973.
4. SCOT Model User's Manual and Program Documentation. Federal Highway Administration, working document, May 1975.
5. H. J. Payne. FREFLO: A Macroscopic Simulation Model of Freeway Traffic: Version I—User's Guide. ESSCOR, Rept. ES-R-78-1, July 1978.
6. H. J. Payne. FREFLO: A Macroscopic Simulation Model of Freeway Traffic, Version I: Program Documentation. ESSCOR, Rept. ES-R-78-2, July 1978.
7. H. J. Payne and D. C. Young. MACK: A Macroscopic Simulation Model of Freeway Traffic. Version II. ORINCON Corp. April 1977.
8. H. J. Payne and H. M. Koble. A Comparison of Macroscopic and Microscopic Simulation Models (MACK and INTRAS). ORINCON Corp. Rept. OC-R-78-11-9367-1, March 31, 1978.
9. M. S. Grewal. Modeling and Identification of Freeway Traffic Systems. Department of Electrical Engineering, Univ. of Southern California, Los Angeles, Ph.D. dissertation, Aug. 1974.
10. D. P. Masher and others. Guidelines for Design and Operation of Ramp Control Systems. Stanford Research Institute, Palo Alto, CA, Aug. 1975, NCHRP Project 3-22.
11. K. M. Hergenrother. Methodology to Generate Fuel Flow Tables for UTCS-1 Traffic Flow Simulation Model. Transportation Systems Center, Cambridge, MA, U.S. Department of Transportation, project memorandum DOT-TSC-05714-PM-76-10, Nov. 1976.
12. H. J. Payne, W. A. Thompson, and L. Isaksen. Design of a Traffic-Responsive Control System for a Los Angeles Freeway. Trans., IEEE, Systems, Man and Cybernetics, Vol. SMC-3, No. 3, May 1973, pp. 213-224.
13. H. J. Payne, W. S. Meisel, and M. D. Teener. Ramp Control to Relieve Freeway Congestion Caused by Traffic Disturbances. TRB, Transportation Research Record 469, 1974, pp. 52-64.

Discussion

E. Hauer and V. F. Hurdle, University of Toronto

To examine the validity of the FREFLO package, we used it on a simple example: a freeway section with no ramps and a bottleneck in its middle. The entering travel demand had a peak that exceeded the capacity of the bottleneck for an appreciable length of time (Figure 18).

The freeway has been divided into 15 sections 1 km (0.6 mile) long. Section 9 served in both cases as a bottleneck; in case 1 the bottleneck was due to a capacity restriction, in case 2 to a lane drop. The demand pattern used is artificially simple but still representative of demand served by urban freeways. It was further assumed that it is appropriate to use the default values built into FREFLO. This is probably equivalent to assuming that the example freeway is similar to the Harbor and Hollywood Freeways in Los Angeles, which seem to form the empirical basis of FREFLO.

The initial conditions were selected to ensure a steady state; the velocity was specified as 88 km/h (55 mph) and the density was selected to satisfy the equation flow = density × speed.

Regardless of the numerical values of speed, flow, and density that the program might generate, we expected to observe the following general features:

1. When the demand exceeded the capacity of section 9, it would become a bottleneck and begin to flow at capacity;
2. Once the bottleneck reached capacity, a congested region of high density and low speed would begin forming upstream of section 9;
3. After demand dropped below the capacity of section 9, the extent of the congested region would begin to diminish;
4. The flow in the bottleneck would remain at capacity until the congestion upstream had cleared; and
5. The flow downstream of section 9 would never exceed the capacity of the bottleneck.

None of this happened. In all test runs, the model produced bottleneck flows substantially in excess of the specified bottleneck capacity for long periods of time. There is no indication of congestion upstream of the bottleneck, nor does the bottleneck restrict flow in sections 10 and beyond.

In short, the output we obtained does not seem to reflect what really happens even in a qualitative manner. There may be three reasons for our failure to obtain sensible results from the FREFLO model.

First, we may have made a mistake in preparing the input. This is somewhat unlikely in view of the simplicity of the input and the fact that we managed to reproduce exactly the results of the example provided in the paper. The latter fact also seems to diminish the possibility that the version of FREFLO we used is faulty.

Second, the program may contain some easily corrigible "bug". We hope that Payne in his closure can demonstrate that, indeed, the problem was of the first

Figure 18. Geometry, capacity, and travel demand for test cases 1 and 2.

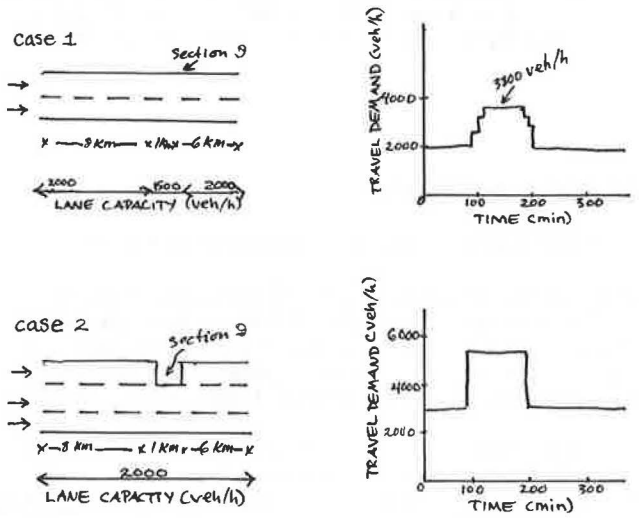

or second kind and that, when used on the above simple test examples, FREFLO can be shown to produce sensible results without any need to tamper with the TEE and VEE parameters.

Third, the program may be built on a faulty theoretical foundation. Whether this is in fact so cannot be ascertained without either Payne's help or a reexamination of the program statement by statement. Consequently, we can only comment on two points that may serve to explain the difficulties we encountered.

The difficulties with the test runs seem to stem from the failure of the program to recognize that there is a bottleneck. Payne uses the term "nominal capacity". This is defined to be "the largest volume that can be sustained under spatially and temporally uniform conditions". He cautions, "It should be realized, however, that under nonuniform conditions, e.g., in the vicinity of a geometric bottleneck, volumes may exceed nominal capacity". It is certainly true that the flow on any highway can exceed its capacity, for a short period of time. However, the possibility of flows exceeding the capacity of a section by 40 percent for 80 min, as in case 2, runs counter to the very definition of capacity. Specifically, if there is congestion upstream of a bottleneck, the average flow in the bottleneck is its capacity.

Another plausible fundamental cause for the apparent failure of FREFLO to replicate traffic flow on a freeway may lie in a common misconception caused by the mathematical formulation of the process (2, 14). Theorists of traffic flow have failed to emphasize sufficiently the discontinuity in the process that occurs at the instant at which a freeway section reaches capacity. This has misled some students of the theory into believing that congestion arises mainly from some instability in the microscopic car-following behavior. In contrast, we believe that freeway congestion arises because travel demand exceeds the capacity of bottlenecks.

Papers that describe computer programs are notoriously difficult to discuss. We can only point to difficulties encountered and speculate about possible explanations. It is hoped that Payne in his closure will be able to demonstrate (using the same test examples) that FREFLO is capable of producing sensible answers about speed, flow, and density under conditions when demand exceeds capacity.

REFERENCE

14. L. Isaksen and H. J. Payne. Freeway Traffic Surveillance and Control. Proc., IEEE, Vol. 61, No. 5, May 1973.

Author's Closure

Before addressing the issues raised in the discussion, it is useful to state the purpose of the paper: to bring to the attention of the traffic engineering community a potentially useful tool for design and evaluation of freeway operational procedures.

It was noted in the paper that model validation efforts have been limited (though promising), and, as they did not yet form a sufficient basis for establishing the validity of the model, they were not described in any detail. I will elaborate here somewhat on these efforts.

In addition to my use of the model in various forms, over the past 10 years, two substantial research projects have employed it. In each case, a limited model-validation effort preceded application. One of these projects was the FHWA-sponsored study on Control Strategies in Response to Freeway Incidents.

In that study, the model parameters were successfully identified to achieve agreement with predictions made by the microscopic simulation model INTRAS (1). In the second, more recent, NCHRP study, model parameters were again successfully identified to gain excellent correspondence with each of four different real-traffic scenarios, two that used Los Angeles data and two Dallas data. Discussions of this effort will be available in the final reports from that project.

The parameters adjusted to achieve agreement in each case involved the section nominal capacities, which were found to be in the range of 1600-1800 vehicles/lane-h.

The purpose of the discussion appears to be to suggest that the model may have fundamental shortcomings. This suggestion is based on a single execution of the model for a simple scenario that produced predictions that, I would agree, are not even qualitatively meaningful.

One will note the contrast between the nature of the validation efforts I have described and the counterexample produced by Hauer and Hurdle. In the former efforts, an attempt was made to adjust parameters to achieve agreement with another simulation or real surveillance data.

The specific shortcomings of the example presented in the discussion is that the nominal section capacities selected (2000 vehicles/lane-h) are too large. The choice made by Hauer and Hurdle may have resulted from too close an association between the model parameters' nominal capacities and the traditional concept of roadway capacity. The model does not directly impose a capacity. Rather, capacity depends on model parameters, including the nominal capacity, and on local spatial variations in density. Thus, in order to obtain a capacity that is sensible—or that corresponds to observations—it is generally necessary to adjust the model parameters.

Generally, one finds the appropriate value of the model parameter nominal capacity to be 10-20 percent less than the capacity observed under ordinary circum-

stances. The discrepancy in the example of the discussion, 28 percent of the maximum flow rate observed (i.e., the capacity), is larger than generally observed. However, this discrepancy is decreased by appropriate selection of other model parameters (k_τ and k_ν as defined by $T_j = k_\tau \Delta x_j$ and $\nu_j = k_\nu \Delta x_j$, respectively. Such adjustments—that is, reduction of the nominal capacity and decreases in k_τ and k_ν—will yield a lower value of roadway capacity and, consequently, produce the effects expected by Hauer and Hurdle.

Publication of this paper sponsored by Committee on Freeway Operations.

Evaluation of the I-35 Route Redesignation in San Antonio

Willam R. Stockton, Conrad L. Dudek, and Donald R. Hatcher,
Texas Transportation Institute, Texas A&M University, College Station

This paper presents the results of studies conducted in San Antonio, Texas, to evaluate the effectiveness of the redesignation of I-35 to an alternate freeway route. The redesignation was designed as a temporary measure to reroute traffic from a congested freeway to one with adequate available capacity. Therefore, only the advance guide signs and gore signs on the approaches to the diversion points were modified. Diversion potential was estimated by using planning-survey and license-plate origin-destination data. Changes in route choice were identified through license-plate origin-destination studies. Mailed questionnaires used to identify characteristics of through and diverting drivers indicated that, although not all through drivers were expected to divert, a significant number shifted from their original routes.

The Texas State Department of Highways and Public Transportation (SDHPT), working in cooperation with the San Antonio Corridor Management Team (CMT), has initiated programs aimed at alleviating congestion and reducing accidents on I-35 in San Antonio near the central business district (CBD). Included among the programs are (a) the redesignation of the I-35 route around the CBD and (b) use of changeable message signs for incident management and freeway diversion.

The Texas Transportation Institute (TTI) was contracted to evaluate the effectiveness of these two programs as part of research sponsored by the Federal Highway Administration (FHWA) on human factors requirements for real-time motorist information displays. In this paper the effects of the I-35 route redesignation are evaluated.

BACKGROUND

Facility Description

The Interstate and other major highway routes through and around the San Antonio metropolitan area are shown in Figure 1. I-35 in San Antonio is the major facility in the Austin-Laredo corridor. It also forms the western and northern boundaries of the CBD. This section of the freeway was completed in 1957. Design standards at the time, coupled with the presence of major drainage tributaries and proximity to the CBD, dictated sharp horizontal alignment of the four-lane facility. Retaining walls and rigid structures prohibit expansion along the existing roadway surface. Because of capacity constraints and alignments, considerable congestion and relatively high accident rates are experienced (1).

I-10 in the southeast part of the city and I-37 were constructed in the late 1960s and early 1970s as eight-lane facilities according to higher design standards. The I-10/I-37 route around the CBD has considerable available capacity and is seldom congested.

Object of I-35 Route Redesignation

The object of the route redesignation was to encourage through drivers in the I-35 Austin-Laredo corridor to travel on the wider I-10/I-37 route in order to reduce congestion and accident rates on I-35. The redesignation was designed as a temporary measure until I-35 could be reconstructed. The I-35 route from the I-35/I-10/US-90 interchange to the I-35/I-37 interchange is about 7.7 km (4.8 miles). The I-10/I-37 route is about 9.0 km (5.6 miles), 1.3 km (0.8 mile) longer.

Sign Changes

SDHPT modified the advance guide signs and gore signs on the freeway sections shown on Figure 2. The sign modifications, completed in November 1977, included moving the destination names (Austin or Laredo) and the I-35 shields so that northbound (NB) and southbound (SB) I-35 traffic would follow the I-10/I-37 route around the CBD. Figure 3 illustrates a typical signing change, which was made at the NB I-35 exit to eastbound (EB) I-10.

For ease of discussion, the two routes will be referred to as route A and route B throughout the remainder of this paper. Route A is the original I-35 route; route B is the newly redesignated route that follows I-10/I-37 around the CBD (see Figure 2).

Study Scope

This study addresses only NB travel in terms of on-site data collection and questionnaires. Cost constraints limited the field data collection to only one direction, and NB was chosen because more appropriate data-collection sites existed there. Some overall conclusions about SB travel are drawn when appropriate.

For the purposes of this study, a through trip is any trip whose origin and destination require that the vehicle